RASĀYAN *J. Chem.*
Vol. 19 | No. 3 | 1654-1665 | July-September | 2026
ISSN: 0974-1496 | e-ISSN: 0976-0083 | CODEN: RJCABP
http://www.rasayanjournal.com
http://www.rasayanjournal.co.in

EVALUATION OF *Prosopis cineraria* LEAF POWDER AS A LOW-COST BIOSORBENT FOR HEAVY METAL REMOVAL FROM WASTEWATER

S. Kumar[1], N. Phogat[1], S. Gandash[2], and A. Yadav[3,✉]
[1]Department of Vocational Studies and Skill Development, Central University of Haryana
Jant-Pali, Mahendergarh-23031, Haryana, India
[2]Department of Chemistry, Suraj Degree College, Gurgaon,122101, Haryana, India
[3]Department of Environmental Studies, Central University of Haryana
Jant- Pali, Mahendergarh-123031, Haryana, India
✉Corresponding author: yadavanoop@rediffmail.com

ABSTRACT
This research evaluates the potential of *Prosopis cineraria* leaf powder as an efficient and cost-effective biosorbent for the elimination of Chromium (Cr^{6+}) and Lead (Pb^{2+}) ions from aqueous media. A series of batch adsorption experiments was conducted to examine the influence of key parameters such as pH, contact time, and initial metal ion concentration on biosorption efficiency. The adsorption characteristics were analysed using both the Langmuir and the Freundlich isotherm models, with the Freundlich model providing a better fit, indicating heterogeneous adsorption sites on the biosorbent surface. Optimal biosorption conditions were identified at pH 4 for Pb^{2+} and pH 5 for Cr^{6+}, with corresponding contact times of 90 minutes and 150 minutes, respectively, using a biosorbent dose of 10 g/l. The maximum adsorption capacities were recorded as 5.22 mg/g for Pb^{2+} and 4.04 mg/g for Cr^{6+}, with corresponding adsorption efficiencies of 75.39% and 70%, respectively. Kinetic studies and regeneration experiments confirmed the reusability of the biosorbent, particularly with successful desorption using HCl, highlighting its potential for sustainable application. The results underscore the viability of *Prosopis cineraria* leaf powder as an eco-friendly and sustainable alternative to conventional adsorbents, which harmonise with the United Nations Sustainable Development Goals. Specifically, the findings support SDG-6 by offering a low-cost, accessible solution for water purification, SDG-12 by promoting the reuse of natural biomass, and SDG-13 by mitigating pollution impacts linked to industrial effluents. This work paves the way for greener technologies in environmental remediation and responsible resource management.
Keywords: Sustainable Development Goals, Biosorption, Heavy Metal Removal, Water Purification, Adsorption Mechanism.

RASĀYAN *J. Chem.*, Vol. 19, No.3, 2026

INTRODUCTION

Among the natural resources, water is the most important element for human survival and the survival of other living things on the planet. The use of water has grown significantly along with the advancement of urbanisation and industrialisation, resulting in a shortage that is impeding economic development.[1] Water pollution has grown to be a global problem at the same time, especially when it comes to heavy metal (HM) poisoning. One major worry for human health and the environment is the presence of heavy metal contamination in industrial wastewater. These metals can build up in living things and disturb ecosystems. They include chromium, zinc, iron, mercury, aluminium, manganese, cobalt, nickel, copper, and lead.[2] Heavy metals can be categorised as necessary, unnecessary, less hazardous, and highly toxic based on their health effects. Some, like copper and zinc, are essential in small amounts but can be hazardous in excess. Others, like mercury, chromium and cadmium, are highly toxic and non-essential. Mercury is known to cause Minamata disease, a neurological condition; copper, zinc, lead, cadmium, and chromium are known to produce Wilson's disease (genetic); these elements can also induce immunological poisoning, bone disorders, diarrhoea, and respiratory problems.[3] Prolonged contact with harmful HMs such as mercury, arsenic, and lead through tainted water can cause serious long-term health problems, such as neurological diseases, cancer, and renal failure. Untreated wastewater used for irrigation also

leads to agricultural issues and soil contamination. It may lower soil fertility and cause toxic compounds to build up in crops, endangering the safety of food.[4] Climate change is also exacerbated by the release of untreated wastewater, which releases greenhouse gases, including nitrous oxide and methane. The absence of wastewater treatment facilities in many developing nations is a significant obstacle that threatens the attainment of the Sustainable Development Goals (SDGs) for environmental sustainability, safe drinking water, and health.[5] Certain conventional techniques for heavy metal removal are: Reverse osmosis, membrane filtration, precipitation using chemicals, exchange of ions, and electrochemical treatment. Some of the drawbacks of these methods are high operating expenditure, electricity consumption, sludge creation, and the requirement for complex infrastructure, notwithstanding their effectiveness.[6] This has sparked a global need for sustainable and community-scalable alternatives, especially those that can solve the water issue while adhering to the values of social justice, economic viability, and environmental preservation. According to the 2030 Agenda for Sustainable Development, the UN approved the SDGs in 2015, which highlight the urgency of this issue.[7] SDGs emphasised the water quality, environmental health, and sustainable technological innovation. The SDG-6 (Clean Water and Sanitation) is to guarantee access to sustainable and safe water sources by enhancing water quality through pollution reduction, hazardous discharge prevention, and chemical waste management from industrial and agricultural sources. SDG-12 (Responsible Consumption and Production) promotes sustainable behaviours that raise living standards by employing renewable natural resources like plant biomass, adopting eco-friendly infrastructure and reducing pollution. The direct effect of water quality on human health is highlighted by SDG-3 (Good Health and Well-Being), since serious illnesses like cancer, neurological disorders, renal damage, and developmental problems in children can be caused by long-term exposure to HMs. Furthermore, SDG-13 (Climate Action) encourages the use of eco-friendly, carbon-neutral technologies that preserve biodiversity, reduce ecological damage and improve climate resilience. Considering this, biological methods, particularly the application of plant-based biosorbents, are being researched as environmentally friendly substitutes for conventional water treatment techniques.[8] Adsorption method is the most affordable, practical, and effective approach that may be used to eliminate HMs from wastewater that is produced by industry without producing any negative impact.[9] Due to their renewability, richness, and intrinsic biochemical qualities, leaf powders from arid-native trees and shrubs are particularly interesting among the several biosorbents that have been studied. *Prosopis cineraria*, also referred to as Khejri, is a tough, drought-resistant plant that is widely distributed in the Middle East and the Indian subcontinent.[10] Adsorption using low-cost materials like *Prosopis cineraria* leaf powder is an eco-friendly and economical alternative. In recent research, several functional groups, including hydroxyl (-OH), carboxyl (-COOH), and amine ($-NH_2$), have been found in its leaf biomass. These groups aid in the binding of HM ions through complexation, ion exchange, and electrostatic interactions. The leaf powder of *Prosopis cineraria* (PCLP) is a powerful biosorbent to eliminate HMs because these chemical groups serve as active sites for metal ion adsorption.[11] Most notably, the applicability of various treatment approaches with lower metal concentration becomes expensive.

Therefore, the employment of easy-to-use and efficient technologies that make use of local resources is a prerequisite when deciding on a treatment plan. For wastewaters contaminated by metals, low-cost methods that facilitate recovery and prevent additional waste creation are gaining grip.[12] Activated carbon is the most common and extensively utilised adsorbent in wastewater treatment, yet it is still a costly material since higher-quality activated carbon is more expensive. Due to cost inefficiency, this circumstance renders it unappealing for widespread application in small-scale companies.[13] However, the application of *Prosopis cineraria* leaf powder for wastewater treatment, specifically for the exclusion of HMs through adsorption, is one of the most effective and widely used techniques. Beyond its effectiveness in the lab, PCLP's potential as a scalable and sustainable solution is demonstrated by its use in actual wastewater situations. It provides the twin benefits of waste valorisation and environmental clean-up[14] because in this study, we use the plant material that would be either thrown out or burned. In addition, unlike certain chemical treatments, it is non-toxic, so it doesn't add new contaminants to the treated water. The application of PCLP is concordant with several green chemistry and circular economy tenets from a sustainability standpoint. It lessens dependency on non-renewable resources and secondary contamination, and encourages the reuse of natural waste products. Furthermore, these findings encourage

the use of inexpensive, user-friendly, and environmentally sensitive community-based water filtration technologies. Such systems have significant socioeconomic benefits, especially in regions with a scarcity of clean water and contemporary purification methods.[15] This study explores the efficacy of *Prosopis cineraria* as an effective, low-cost absorbent for the elimination of toxic HM, especially Cr (VI) and Pb (II), from aqueous solutions. This investigation aims to address persistent environmental concerns associated with heavy metal contamination by evaluating the absorption capacity and efficiency of *Prosopis cineraria* leaf powder.

EXPERIMENTAL

Preparation (*Prosopis cineraria* leaf powder)

Prosopis cineraria leaf samples were collected from the upper matured and physically undamaged portions of the tree from various locations around the university campus. To remove any soluble impurities and dirt, tap water was used. *Prosopis cineraria* leaves were sun-dried for five days or until they were crisped. After five days of sun drying, leaves were further dried in a hot air oven for 24h at 50°C. The dried leaves were ground using a grinding mixer. The *Prosopis* leaf powder was sieved with a mesh size of 2 mm to produce a biosorbent with a size of 1 to 2 mm and packed in a glass bottle.

Preparation of HM (synthetic) Solution

The wastewater containing HMs used in the study was artificially prepared in a laboratory. This method was needed because it can be challenging to separate the impacts of particular metals due to the presence of other soluble and insoluble components in actual wastewater, which might affect how metals adsorb onto tree leaves. Single metal ion was dissolved in reliable experimental conditions in each wastewater sample. The metal crystals were dissolved using distilled water. This was also done to eliminate any potential interference from other soluble substances that could be present in regular tap or drinking water. Within this experiment, a stock solution of Cr^{6+} and Pb^{2+} was prepared using the salts of potassium dichromate ($K_2Cr_2O_7$) and lead nitrate (Pb $(NO_3)_2$).

Chromium (VI) Solution

This solution has been made taking 1.414 g of $K_2Cr_2O_7$ in 500 ml of double-distilled water as 1000mg/l of Cr^{6+}. It was used to make synthetic samples with different chromium contents each time by using the appropriate dilution. To alter the pH of the solution, the 0.1N amounts of each HCl and NaOH required were adjusted.

Lead (II) Solution

This solution was made using 0.7992 g of Pb (NO_3) in 500 ml of double-distilled water as 1000 mg/L of lead metal. It was used to make synthetic samples with different lead concentrations each time by using the appropriate dilution.

Experiment Design

The study conducted batch sorption experiments to evaluate the adsorption efficiency of *Prosopis cineraria* leaf powder (PCLP) for the extraction of Pb^{2+} and Cr^{6+} ions from synthetic solutions. Batch experiments were completed by adding 0.5 g of PCLP to 50 mL of metal ion solutions through conical flasks, followed by agitation in an orbital shaker at 200 rpm for 24 hours. Optimization of parameters, including pH (2–8), adsorbent dosage (5–80 g/L), IMC (10–60 mg/L), and contact time (30–180 min), was performed by varying one parameter at a time while keeping others constant. At predetermined time intervals, samples were withdrawn, filtered using Whatman paper No. 1, and digested by heating with 1.0 mL HNO_3 and 0.5 mL HCl at 95°C until the colour was removed. The concentrations of residual metal ions in the filtrate were measured using Atomic Absorption Spectrophotometry (Lab India, AA8000). Metal ions removal percentage was determined using the equation:

$$\text{Adsorption Efficiency (\%)} = (Co - Ce/Co) \times 100$$

Where Co is the initial concentration (mg/L), and Ce is the final concentration (mg/L) of metal ions.
The adsorption capacity q_t(mg/g) of PCLP was determined using:

$$q_t = (Co - Ce) \times V/M$$

Where V is the volume of the metal solution (mL), and M is the mass of the biosorbent (g)

RESULTS AND DISCUSSION

Impact of Variables

The impacts of variables, such as contact time, pH, and Initial Metal Ion Concentration (IMC) in the aqueous solution, on metal ion adsorption were evaluated in several batch investigations.

Effect of pH

Various factors, such as metal ion solubility, counter ion concentration, interactions with adsorbent functional groups, and adsorbate ionisation during the adsorption process, were all significantly influenced by pH in the context of metal ion removal from aqueous solutions.[16] For the study of the effect of pH on adsorption, we have taken six pH levels (i.e., 2, 3, 4, 5, 6 and 8). During the study, different phases was seen with the change in the pH on PCLP-mediated Pb^{2+} and Cr^{6+} adsorption (Fig.-1a, b). The adsorption of Pb^{2+} was lowest at pH 2–3, where excess H^+ ions compete with Pb^{2+} for active sites on the biosorbent, leading to reduced adsorption. As the pH increases, the biosorbent surface becomes more negatively charged, enhancing Pb^{2+} binding. A maximum adsorption percentage of 99.37% was observed at pH 4 for Pb^{2+}. Beyond pH 4–6, the adsorption remains relatively stable, followed by a slight decline at higher pH values. This observation aligned with previous studies. Using *Prosopis cineraria* leaf powder and response surface methods, Namdeti et al[11] showed that Pb^{2+} was removed by about 83.77% at an optimal pH of 4.7. In the case of Cr^{6+}, adsorption was low at pH 2–3 and increased with increasing pH, achieving a maximum adsorption percentage of 98.77% at pH 5. This was due to strong electrostatic attraction between protonated biosorbent sites and anionic species like $HCrO_4^-$. Beyond pH 5, adsorption slightly declines and stabilises, indicating mildly acidic pH favours Cr^{6+} removal. The Cr^{6+} adsorption peak at pH 4–5 using *Prosopis cineraria* leaf powder aligns with Ali et al[17], who reported maximum removal at lower pH using amide-modified biochar. This difference was due to stronger protonation of functional groups in modified biochar at lower pH.

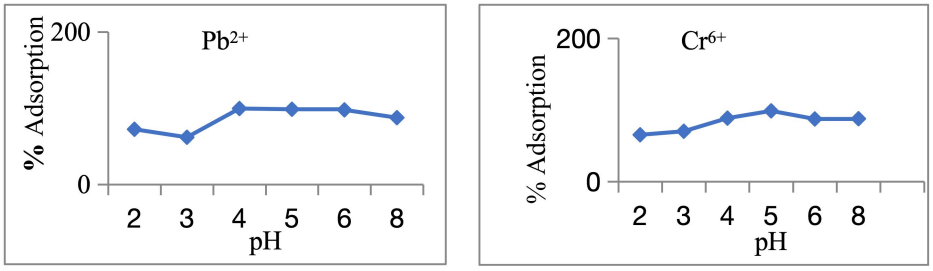

Fig.-1: (a) Impact of pH on Pb^{2+} Adsorption using PCLP, (b) Impact of pH on Cr^{6+} Adsorption using PCLP

Impact of Contact Time

The equilibrium time needed for adsorption of Pb^{2+} and Cr^{6+} ions on the PCLP was studied at different time intervals (30, 60, 90, 120, 150 and 180 min), keeping all other parameters constant (i.e. pH, initial concentration as in Fig.-3. Adsorption of Pb^{2+} increased rapidly with time, reaching a maximum of 97.4% at around 90 minutes, which was the optimal contact time. Higher active sites on the biosorbent surface increase the rapid intake of HMs. The adsorption slightly declined or stabilised after 90 minutes, indicating that equilibrium had been achieved. Compared to the present study, the pineapple peel biosorbent used by Saraswaty *et al.*[18] showed much faster Pb^{2+} adsorption, achieving over 90% removal within 0.5 minutes, while *Prosopis cineraria* leaf powder took around 90 minutes for 97.4% removal. Compared to the present study, Indra *et al.*[19] reported a slower Pb^{2+} adsorption process, achieving 92.92% removal at 240 minutes using a clay–carbon–manganese monolith, while *Prosopis cineraria* leaf powder reached 97.4% removal in just 90 minutes. In the case of Cr^{6+}, adsorption showed a slower and more gradual increase, reaching a peak of 85.92% adsorption at around 150 minutes, which was the optimal contact time. This slower rate might be due to diffusion into internal pores or redox interactions. After this point, adsorption levels off, indicating that equilibrium had been established. The Cr^{6+} adsorption trend in the present study, which reached equilibrium around 150 minutes, aligns closely with other studies that reported the tannin-immobilised goat hair achieves equilibrium in 200 minutes under similar conditions.[20]

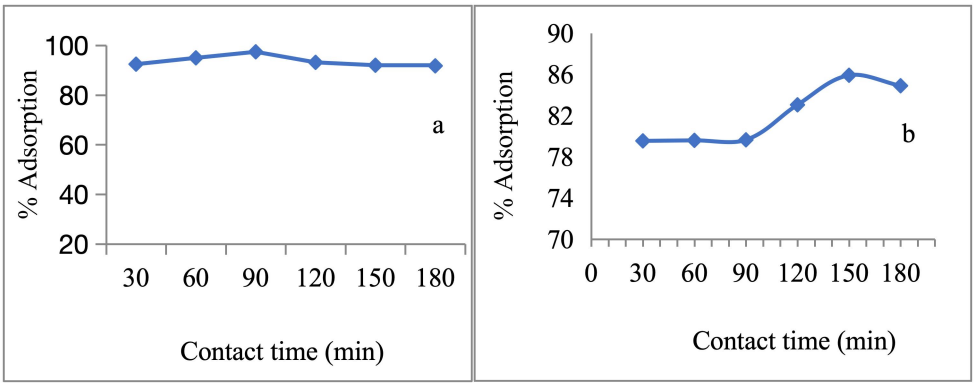

Fig.-2: (a) Contact Time Impact on Pb^{2+} Elimination on PCLP, (b) Contact Time Impact on Cr^{6+} Elimination on PCLP

Impact of Initial Metal Concentration

The effect of IMC played a significant role in adsorption behaviour. The total amount of metal adsorbed typically increased due to elevated initial metal ion concentration, showing mass transfer between the aqueous phase and the adsorbent surface. However, the percentage removal often decreased because the fixed number of available adsorption sites becomes saturated at higher concentrations.[21] For both chromium and lead, Krishan and Anirudhan[22] observed that the amount of metal adsorbed rose with concentration up to 10 mg/L, and after this level, the biosorbent sites begin to approach saturation. Similarly, adsorption efficiency tends to plateau or decline when the concentration exceeds 20 mg/L due to limited binding site availability. According to Senthil *et al.*[23], the percentage adsorption decreases with increasing metal ion concentration due to the limited number of available adsorption sites on the biosorbent surface. Although the total amount of metal ions adsorbed increases at higher concentrations due to a stronger concentration gradient overcoming mass transfer resistance, the percentage removal declines. This was because at lower concentrations (10 mg/L), more adsorption sites were available relative to the number of metal ions, resulting in higher adsorption efficiency. At higher concentrations, site saturation occurs, leading to lower percentage adsorption for both Pb^{2+} and Cr^{6+}. In both cases, as shown in Fig.-3(a) for Pb^{2+} and Fig.-3(b) for Cr^{6+}, the percentage adsorption decreased as IMC raised from 10 mg/L to 60 mg/L. Over the same concentration range, for Pb^{2+}, the adsorption drops from approximately 85% at 10 mg/L to about 55% at 60 mg/L, while for Cr^{6+}, it decreased from around 84% to 53%. This decline was attributed to the saturation of available adsorption sites on the PCLP surface. At lower concentrations, a greater number of active sites were available, resulting in higher adsorption efficiency. However, as the concentration increased, the fixed number of active sites became insufficient, leading to reduced percentage removal. The results observed in the present study aligned closely with the findings reported by Fasoto *et al.*[24], where the adsorption of metal ions (specifically Zn^{2+} and Cr^{6+}) onto sugarcane pulp also displayed a decline in percentage adsorption with increasing initial metal ion concentration. In both studies, this trend was observed due to the limited active adsorption sites on the biosorbent surface.

Adsorption Isotherm

The adsorption isotherms effectively represent the correlation between the amount of Pb^{2+} and Cr^{6+} adsorbed and their equilibrium concentrations in the aqueous phase. As illustrated in Fig.-4(a) and 4(b), the adsorption capacity for both $Pb^{2+}$and Cr^{6+} increased proportionally with the IMC, ranging from 10 to 60 mg/l. The characteristic shape of the curves at all tested temperatures corresponds to an L-type isotherm, indicating a high affinity between the adsorbate and adsorbent, and reflecting a typical Langmuir-type monolayer adsorption behaviour at equilibrium.

Cracking the Langmuir Isotherm

According to the Langmuir adsorption isotherm model, a homogeneous adsorption surface with a finite number of identical sites leads to monolayer adsorbate coverage. This model assumed uniform adsorption energy and no interaction between adsorbed molecules.[25]

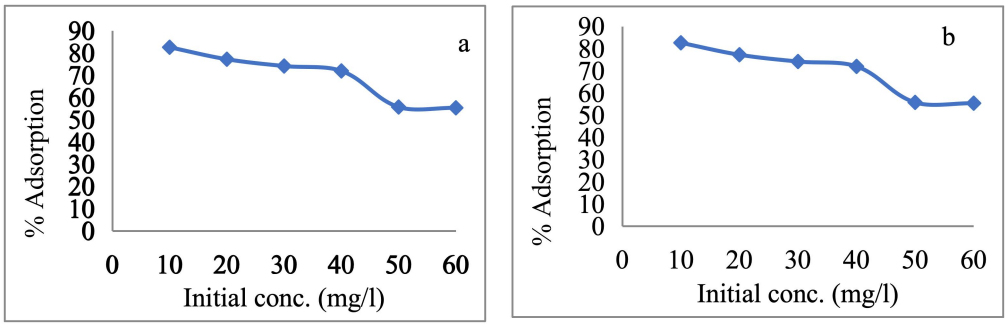

Fig.-3: (a) Impact of IMC of Pb^{2+} on PCLP, (b) Impact of IMC of Cr^{6+} on PCLP

Langmuir equation's linearised form was expressed as:

$$[C_e/q_e = 1/K_L q_m + C_e/q_m]$$

Here, q_m (mg/g) represents the maximum monolayer adsorption efficacy, and K_L (L/mg) denotes the Langmuir constant related to the affinity of the binding sites. Figures-4(a) and 4(b) presented the linear Langmuir plots for Pb^{2+} and Cr^{6+}, respectively. The slope and intercept of these plots were used to conclude the Langmuir constants. For Pb^{2+}, the slope ($1/q_m$) was 0.1916, and the intercept ($1/K_L q_m$) was 0.5206, yielding a calculated maximum adsorption capacity qm of 5.22 mg/g and a Langmuir constant KL of 0.368 L/mg. Similarly, for Cr^{6+}, the slope and intercept were 0.2475 and 1.6184, respectively, corresponding to a q_m of 4.04 mg/g and K_L of 0.152 L/mg. These theoretical values were in strong agreement with the experimentally determined adsorption capacities of 4.814 mg/g for Pb^{2+} and 3.322 mg/g for Cr^{6+}, thereby validating the applicability of the Langmuir model for describing the adsorption behaviour of these metal ions on the biosorbent. The higher K_L value for Pb^{2+} indicated a greater affinity toward the adsorbent surface compared to Cr^{6+} under identical conditions. Furthermore, the separation factor (R_L), expressed by the equation:

$$R_L = 1/1 + K_L C_0$$

It provides insights into the favourability of adsorption. The R_L values for both metals, as depicted in Figures 6a and 6b, decreased with increased initial metal concentrations (10–60 mg/l), indicating highly favourable adsorption ($0<R_L<1$) under all tested conditions. The downward curvature was characteristic of L-type isotherms, further confirming monolayer adsorption behaviour and high adsorbent affinity.

Table-1: Calculated Constant of Langmuir Isotherm Data

Langmuir	Pb^{2+}			Cr^{6+}		
	q_m	K_L	R^2	q_m	K_L	R^2
	5.22	0.368	0.8962	4.04	0.152	0.9816

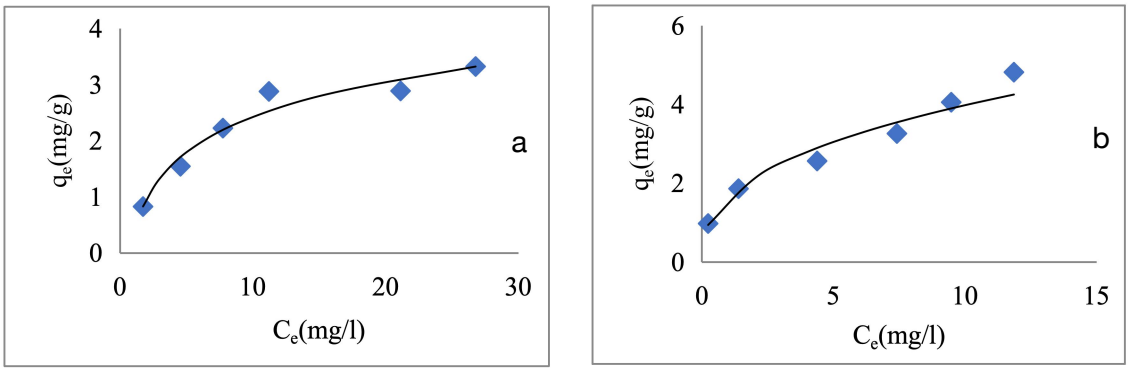

Fig.-4: (a) Pb^{2+} Adsorption on PCLP, (b) Cr^{6+} Adsorption on PCL

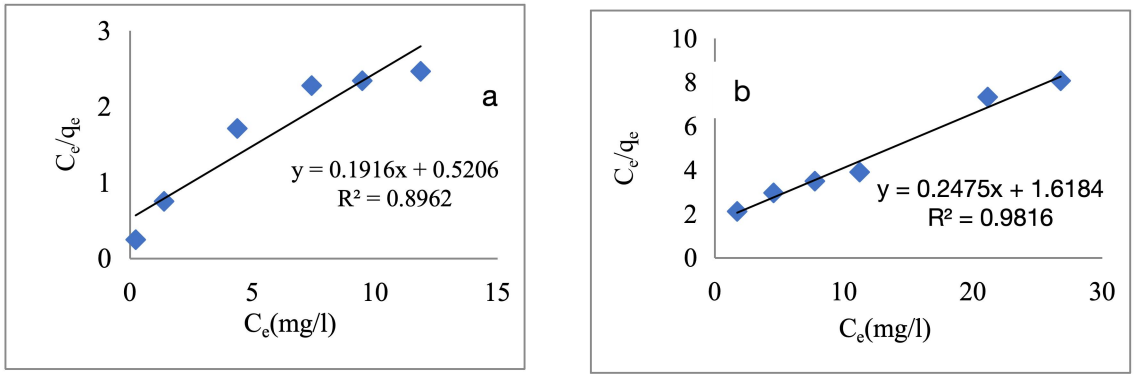

Fig.-5: (a) Pb^{2+} Adsorption on PCLP, (b) Cr^{6+} Adsorption on PCLP

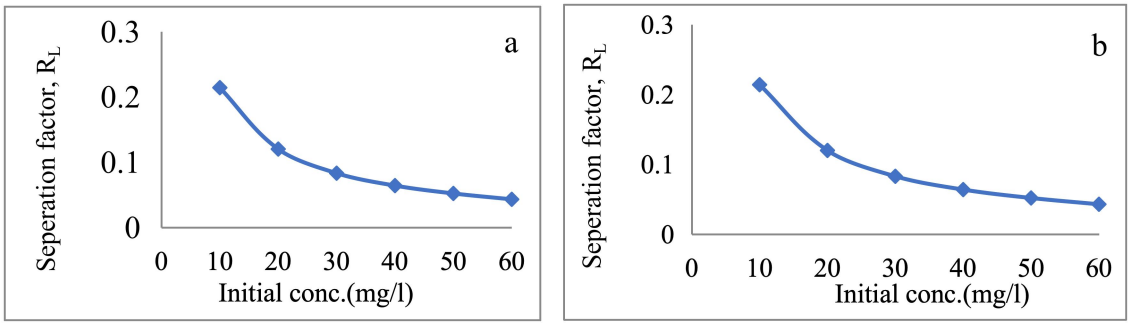

Fig.-6: (a) Determination of Pb $^{2+}$ R_L in Relation to Metal Ion Concentration (mg/l), (b) Determination of Cr^{6+} RL in Relation to Metal Ion Concentration (mg/l)

Freundlich Isotherm

The isotherm model of Freundlich offered a framework that describes heterogeneous adsorption, particularly in systems where adsorption heat was non-uniformly distributed. It assumes multilayer adsorption and variable interaction energies, influenced by the occupation of adjacent adsorption sites.[26] The linearised form of the Freundlich equation was stated as:

[log q_e = log K_f +1/n log C_e]

'Where qe denotes solute adsorbed at equilibrium (mg/g), C_e reflect is the equilibrium concentration (mg/L), K_F represents the Freundlich constant indicative of adsorption capacity, and n is the adsorption intensity. The study was conducted under controlled conditions, such as a temperature of 30°C, a 10 g/L dose of biosorbent, and a 200-rpm speed of an orbital shaker. The Freundlich plots of logq_e versus logC_e for Pb^{2+} and Cr^{6+} (Fig.-7a and b) yielded linear trends from which the constants were derived. For Pb^{2+}, the calculated Freundlich constant K_f was 1.636 mg/g with an adsorption intensity n=2.58, and a high correlation coefficient R^2=0.9764 indicating a strong fit to the model. Similarly, Cr^{6+} showed a Freundlich constant of 0.708 mg/g, n=2, and R^2=0.936, confirming the model's validity for both metal ions. Overall, the results (Table-2) suggest that adsorption of Pb^{2+} and Cr^{6+} onto the biosorbent followed the Freundlich isotherm, with Pb^{2+} demonstrating higher adsorption capacity and a stronger linear correlation.

Table-2: Calculated Constant of the Freundlich Isotherm Data

Freundlich	Pb^{2+}				Cr^{6+}			
	Slope	n	K_f	R^2	Slope	n	K_f	R^2
	0.387	2.58	1.636	0.9764	0.4997	24.04	0.708	0.9363

Adsorption kinetics research revolved around the solute uptake rate, which was important in defining the duration of adsorbate absorption at the 'solid-solution interface'. It also considered the diffusion process. It was essential to comprehend this rate to optimise adsorption operations. Here, we examined the kinetic analysis with particular attention to the ideal pH ranges for Pb^{2+} and Cr^{6+} adsorption, the application of two well-known models, and the adsorption studies' results.

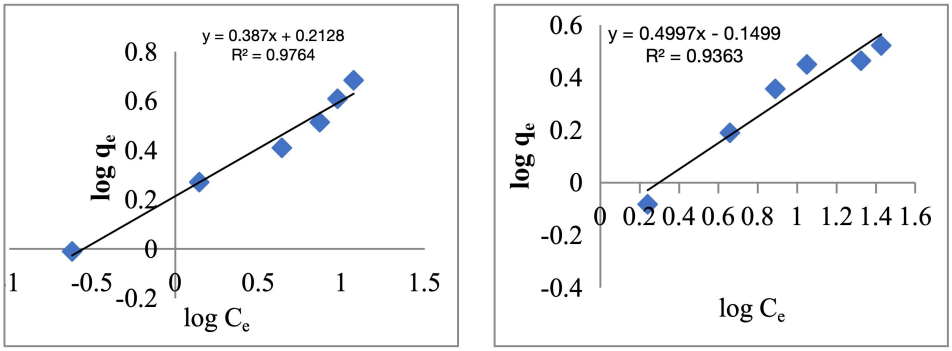

(a) (b)

Fig.-7: (a) Freundlich Isotherm Curve for Pb^{2+} Adsorption on PCLP, (b) Freundlich Isotherm Curve for Cr^{6+} Adsorption on PCLP

The pH Levels that are Ideal for Maximum Adsorption

To maximize Pb^{2+} and Cr^{6+} adsorption efficiency, ideal pH values were essential. The ideal pH for Pb^{2+} adsorption is 4, while the ideal pH for Cr^{6+} adsorption is 5, according to thorough kinetic analysis. The adsorption capacity reached its maximum at these pH values, guaranteeing the best possible removal of pollutants from the solution.

Examining Kinetic Adsorption Models

The adsorption kinetics of Pb^{2+} and Cr^{6+} onto *Prosopis cineraria* leaf powder were studied using pseudo-first and second-order models, respectively. Experiments were conducted using an IMC of 10 mg/L, with contact times varying from 30 to 180 minutes, while all other parameters were maintained constant. These models were used to estimate rate constants and adsorption capacities, providing insight into the adsorption mechanisms and kinetics under controlled conditions. Table-3 depicts the estimated kinetic data for lead and chromium.

Evaluation of Kinetic Information

Pseudo-First Order Model

Plotting pseudo-first-order adsorption kinetics 'log (q_e-q_t) against time (t) results in a linear relationship (Fig.-8a and b). It was easier to determine the 'adsorption rate constant', k_1, because of this linearity. Relative to Cr^{6+}, Pb^{2+} notably showed a higher regression factor (R^2), suggesting a better fit with the experimental data.

Second-Order Pseudo Model

R^2 values greater than 0.9, on the contrary, indicated that the 'pseudo-second-order model' fitted Pb^{2+} and Cr^{6+} adsorption kinetics better. The rate parameters, k_2 and q_e, can be directly determined by looking at the intercept and slope of the plot of t/q_t against time (t) (Figs.-9a and b).

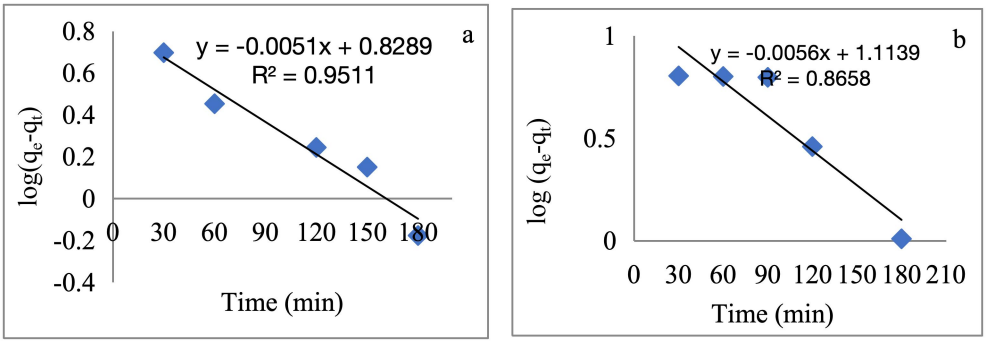

Fig.-8: (a) Sorption Kinetics Plot for Pb^{2+} Ions Removal from Aqueous Media by PCLP, (b) Sorption Kinetics Plot for Cr^{6+} Ions Removal from Aqueous Media by PCLP

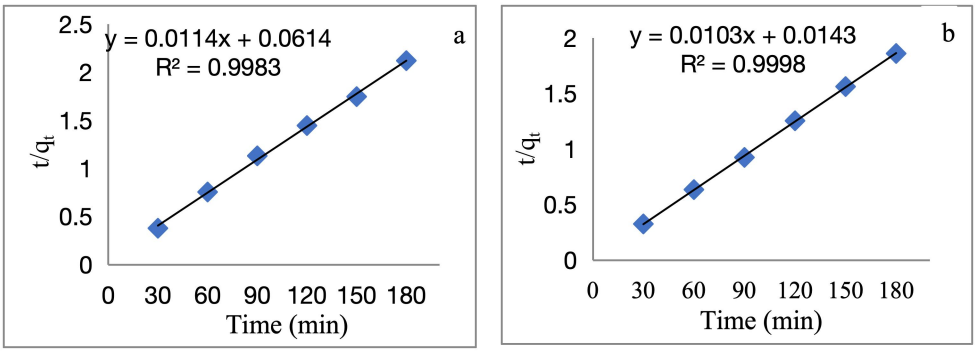

Fig.-9: (a) Sorption Kinetics Plot for Pb^{2+} Removal onto PCLP, (b) Sorption Kinetics Plot for Cr^{6+} Removal Onto PCLP

Table-3: Calculated Constants of Pseudo-First and Second Order Kinetic Models of Lead and Chromium Biosorption

Metal Ion	C_0 (mg/L)	q_1 (mg/g)	k_1 (1/min)	R^2_1 (First Order)	q_2 (mg/g)	k_2 (g/mg·min)	R^2_2 (Second Order)
Pb^{2+}	10	6.74	0.0051	0.9511	87.72	0.00212	0.9983
Cr^{6+}	10	13.01	0.0056	0.8658	97.09	0.00742	0.9998

Desorption Studies

Using double-distilled water, desorption tests were carried out right after the corresponding Pb^{2+} and Cr^{6+} were adsorbed by PCLP. After draining the loaded biosorbent to extract all metal ions from the mixture, it was suspended in 50 millilitres.'1 M HCl, 0.1 M HNO_3, 0.1 M H_2SO_4', and 30 minutes at 30 °C in distilled water. The percentages of Pb (II) and Cr (VI) that underwent desorption ranged from 1.679 to 69.38% and 3.40 to 40.35%, respectively (Fig.-10a and b). Desorption with 0.1 M HCl yields the best result for both metals in the study.

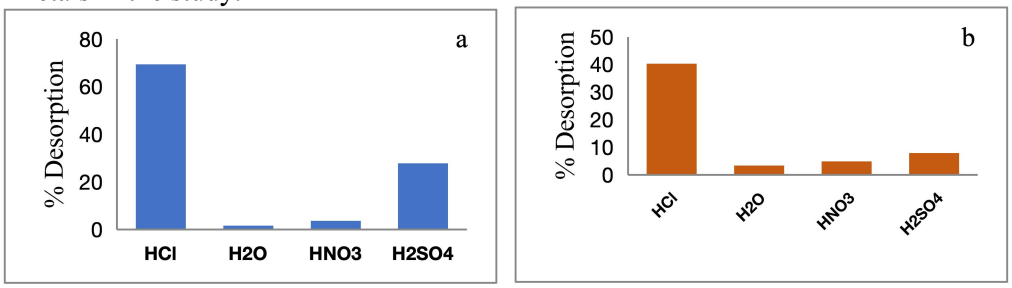

Fig.-10: (a) Percentage of Desorption of Pb^{2+} from PCLP, (b) Percentage of Desorption of Cr^{6+} from PCLP

Scanning Electron Micrography

The Interior morphological structure of the biosorbent was examined using a scanning electron microscope. The SEM micrograph images of PCLP showed a lot of gaps and extremely uneven surfaces, which allow metal adsorption to occur (Fig.-11a). The graphic makes it evident that there were more pores on the surface, which means that there were more sites available for the metal ion adsorption. The morphological structure of PCLP following Pb^{2+} adsorption was depicted in Fig.-11 b, whereas the morphological structure following Cr^{6+} adsorption was shown in Fig.-11c. The pictures demonstrated how the adsorption process attached the metal ions to the pores.

Characterization of Biosorbent Systems

Fourier Transformation Infra-Red (FTIR) Spectroscopy

When confirming the functional unit engaged in the process of 'biosorption of heavy metal' ions on PCLP (polymer-coated lignocellulosic particles), FTIR spectra are an essential tool. The spectra of the native,

Pb^{2+} treated, and Cr^{6+} treated samples are shown in Figures 13a,13b, and 13c, respectively. These spectra's examination shows the existence of important functional groups that are necessary for biosorption. Identified Functional Groups: -OH and -NH Stretching Bands PCLP's FTIR spectra show noticeable broad bands in the 3400–3200 cm^{-1} range, which are suggestive of stretching vibrations of the –OH and –NH atoms.

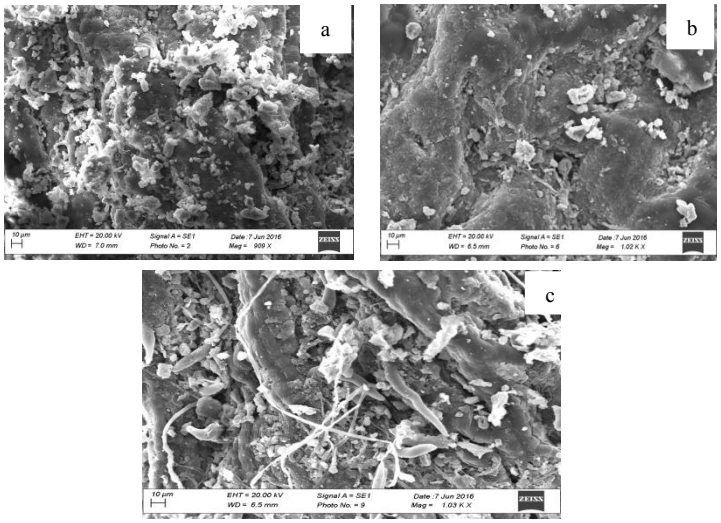

Fig.-11: (a), (b) and (c) Scanning Electron Micrographs of PCLP before Biosorption, after Biosorption of Pb^{2+}, Cr^{6+} Metal Ions, Magnification 1.03 K X, Bar Represents 10µm

Carboxyl Groups

The existence of these functional groups is explained by the stretching band of carboxyl groups in the aromatic ring, which appears as peaks at 1635 cm^{-1}.

Differential Functional Groups

Various functional groups present on PCLP are responsible for the characteristic bands detected at wavenumbers: Polypeptide Structures: C-OH stretching vibrations: 1318 and 1036 cm^{-1}; C-H stretching vibrations: 2918 and 2850 cm^{-1}; $-CH_3$ wagging: 1236 cm^{-1}, C-N-C scissoring is exhibited by polypeptide structures, which contributes to peaks in the spectra that range from 514 to 780 cm^{-1}.

Effects of Metal Ion Therapy

Figures-12 a, b and c illustrate that the FTIR spectra of the biosorbents treated with Pb^{2+} and Cr^{6+} show slightly higher absorption than the native sample. This observation implies that the treatment with heavy metal ions modifies the functional unit of the biosorbent.

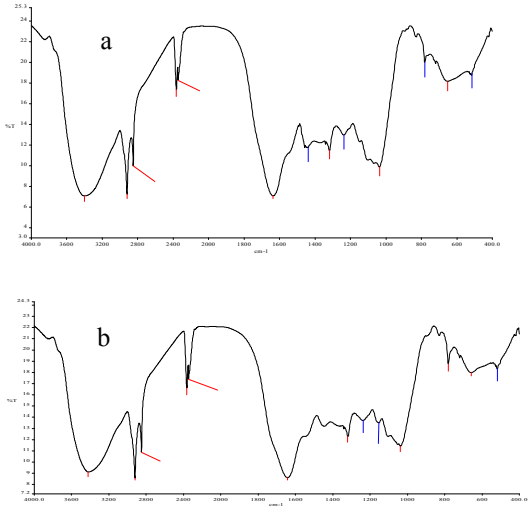

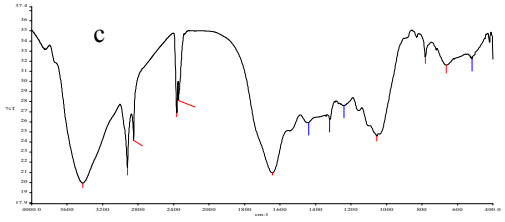

Fig.-12: (a) PCLP's Pre-biosorption FTIR Spectrum, (b) FTIR Spectra of PCLP Pb^{2+} Treated (Pb^{2+}=50mg/l), and (c) FTIR Spectra of PCLP Cr^{6+} Treated (Cr^{6+}:50mg/l)

CONCLUSION

Mature *Prosopis cineraria* leaves are used to create *Prosopis cineraria* leaf powder (PCLP) as a biosorbent. Pb^{2+} and Cr^{6+} have been effectively adsorbed out of their synthesised solutions using the produced leaf powder. Based on the experimental study, the *Prosopis cineraria* leaf powder (PCLP) that has been produced was shown to be more cost-effective and efficient. The optimal pH for Pb^{2+} and Cr^{6+} was 4 and 5, respectively. The ideal adsorption periods for Pb^{2+} and Cr^{6+} were 90 and 150 minutes, respectively. The best concentration of biosorbent discovered during the experimental research was 10 mg/l. As the original metal concentration rose, removal efficiency dropped. As the adsorption (contact) period increases, removal efficiency first rises and then gradually falls. Compared to the 'Langmuir isotherm model', the Freundlich isotherm model provided a better description of the experimental results. For Pb^{2+}, but not for Cr^{6+}, experimental evidence agrees well with pseudo-first-order kinetics. For both metal ions, the experimental finding is in good accord with the pseudo-second-order kinetics. After the HCl treatment, the biosorbent can be renewed and employed again, according to the desorption investigations. *Prosopis cineraria* leaf powder provides an economical and eco-friendly way to extract Pb^{2+} and Cr^{6+} from artificial water-based solutions. The results are aligned with SDG 6 by offering a low-cost, accessible solution for water purification, SDG 12 by promoting the use of natural biomass, and SDG 13 by mitigating pollution impacts associated with wastewater. Human health and the environment are seriously endangered by heavy metals, yet this creative solution appears to be a promising one.

ACKNOWLEDGEMENTS

Authors are thamkful to the authorities of their institutions for the cooperation and support they provided.

CONFLICT OF INTERESTS

The authors declare that there is no conflict of interest.

AUTHOR CONTRIBUTIONS

The present work is closely related to *SDG-6: Clean water and Sanitation*. All the authors contributed significantly to this manuscript, participated in reviewing/editing and approved the final draft for publication. The research profile of the authors can be verified from their ORCID ids, given below:

Sunil Kumar https://orcid.org/0000-0003-3875-2251
Naseeb Phogat http://orchid.org/0000-0001-9667-8067
Sushmita Gandash http://orchid.org/0009-0007-0671-0010
Anoop Yadav https://orcid.org/0000-0001-8719-6410

Cite this article as: S. Kumar *et al.*, *Rasayan J. Chem.*, 19(3), 1654-1665(2026), https://doi.org/10.31788/RJC.2026.1939757

REFERENCES

1. B. Verma and C. Balomajumder, *Environmental Science and Pollution Research*, **27**, 13844(2020), https://doi.org/10.1007/s11356-020-07988-0

2. N. Burnase, S. Jaiswal and A. Barapatre, in: K. Randive, S. Pingle and A. Agnihotri (Eds.), Springer Nature, pp. 127–186 (2022), https://doi.org/10.1007/978-3-030-99495-2_7
3. J. Zhou, Z. Jiang, X. Qin and L. Zhang, *Water*, **16**, 2179(2024), https://doi.org/10.3390/w16152179
4. N. Shabansalmani and A. Javadi, In Proceedings of the 24th International Congress of Microbiology of Iran, Tehran, Iran (2023), https://civilica.com/doc/1921956
5. I. Anazonwu and M. Fahmi, *Recent Advances in Natural Sciences*, **2(2)**, 121(2024). https://doi.org/10.61298/rans.2024.2.2.121
6. S. Rajoria, M. Vashishtha and V. K. Sangal, *Environmental Science and Pollution Research*, **29**, 72196(2022), https://doi.org/10.1007/s11356-022-18643-y
7. G. Gratzer and W. Keeton, *Mountain Research and Development*, **37**, 246(2017), https://doi.org/10.1659/MRD-JOURNAL-D-17-00093.1
8. O. Kovalenko and A. Kokhanska, *Scientific Works*, **2(85)**, 38(2021), https://doi.org/10.15673/swonaft.v2i85.2160
9. M. Akter, M. Bhattacharjee, A. K. Dhar, F. B. A. Rahman, S. Haque, T. U. Rashid and S. M. F. Kabir, Gels, 7, 30 (2021). https://doi.org/10.3390/gels7010030
10. T. Alizadeh, M. Matinizadeh, H. Habashi and S. M. Sadeghi, *Journal of Wood and Forest Science and Technology*, **29**, 89(2022), https://doi.org/10.22069/jwfst.2022.19948.1962
11. R. Namdeti, B. Gaddala, N. R. Lakkimsetty, N. Qahoor, B. S. Naveen, U. Meka, et al., *Journal of Environmental & Earth Sciences*, **7**, 292(2024), https://doi.org/10.30564/jees.v7i1.7474
12. T. Sen, *Molecules*, **28**, 5575(2023), https://doi.org/10.3390/molecules28145575
13. Z. Djezzar, A. Aidi, H. Rehali, Z. Sabrina and O. Tarik, *RSC Advances*, **14**, 5276(2024), https://doi.org/10.1039/d3ra08678j
14. M. Samimi and J. Nouri, *Global Journal of Environmental Science and Management*, **11**, 391(2025), https://doi.org/10.22034/gjesm.2025.02.02
15. M. A. S. Ansari, M. J. Islam, M. R. Jany, et al., *Journal of Angiotherapy*, **8**, 1(2024), https://doi.org/10.25163/angiotherapy.81210161
16. L. Cruz-Lopes, M. Weber Macena, B. Esteves and R. Guiné, *Open Agriculture*, **6**, 115(2021), https://doi.org/10.1515/opag-2021-0225
17. A. Ali, S. Alharthi, N. Al-Shaalan, A. Naz and H.-J. Fan, *Molecules*, **28**, 5146(2023), https://doi.org/10.3390/molecules28135146
18. V. Saraswaty, E. S. Aji, A. Hanifah, et al., *IOP Conference Series: Earth and Environmental Science*, **1388**, 012032(2024), https://doi.org/10.1088/1755-1315/1388/1/012032
19. H. Indra, D. Darmadi, A. Adisalamun, A. Chairunnisak and R. C. L. Nasrullah, *Elkawnie: Journal of Islamic Science and Technology*, **9**, 188(2023), https://doi.org/10.22373/ekw.v9i2.16976
20. Y. Li, H.-W. Ma and X.-S. Wang, *Journal of the American Leather Chemists Association*, **120**, 171(2025), https://doi.org/10.34314/dxasz540
21. B. Yu, Y. Zhang, A. Shukla, S. S. Shukla and K. L. Dorris, *Journal of Hazardous Materials*, **B80**, 33(2002), https://doi.org/10.1016/S0304-3894(00)00317-8
22. K. A. Krishnan and T. S. Anirudhan, *Water SA*, **29**, 147(2003), https://doi.org/10.4314/wsa.v29i2.4852
23. K. P. Senthil, S. Ramalingam, C. Senthamarai, M. Niranjanaa, P. Vijayalakshmi and S. Sivanesan, *Desalination*, **261**, 52(2010), https://doi.org/10.1016/j.desal.2010.05.032
24. T. Fasoto, J. Arawande and A. Akinnusotu, *International Journal of Scientific and Engineering Research*, **8**, 45(2014).
25. S. Amiri Khoshkar Vandani, R. Fazaeli, M. Giahi Saravani and H. Pasdar, *Egyptian Journal of Chemistry*, **64**, 5803(2021), https://doi.org/10.21608/ejchem.2021.33523.270
26. G. S. Dos Reis, P. S. Thue, B. G. Cazacliu, E. C. Lima, C. H. Sampaio, M. Quattrone, E. Ovsyannikova, A. Kruse and G. L. Dotto, *Journal of Cleaner Production*, **256**, 120416(2020), https://doi.org/10.1016/j.jclepro.2020.120416

[RJC-9757/2026]